Earthquake Engineering, Tenth World Conference © 1992 Balkema, Rotterdam. ISBN 90 5410 060 5

Seismic behavior of steel frames with composite beams by pseudodynamic testing

Kuniaki Udagawa & Hiroaki Mimura
Tokyo Denki University, Japan

ABSTRACT: Earthquake response analysis of two-bay one-story steel frames with and without concrete slabs is performed by pseudodynamic testing. The ground acceleration used in the test simulates that of the El Centro NS earthquake (1940). The influence of the presence or absence of a concrete slab on the seismic behavior of frames is investigated. We also examine how compressive failure of the concrete slab affects the frame and the beam behavior. In addition, the tests reveal the difference in behavior between two types of composite beams, one joined to an interior column and the other to an exterior column. The tests also reveal the relationship between frame ductility and beam ductility. These analyses clarify that the presence of the concrete slab greatly affects the seismic behavior of the frame and beam. Furthermore, the behavior of the frame with a concrete slab is governed by whether or not compressive failure occurs.

1 INTRODUCTION

In most steel frames, steel beams are connected tightly with concrete slabs by shear connectors. The steel beam with the concrete slab is called a composite beam. Frames with such composite beams show complex behavior during an earthquake because of the complicated moment rotation relationship of the composite beams. Numerical analysis methods which study the complex seismic behavior of the frames with composite beams were reported(1,2). However, practical and accurate analytical methods for elastic-plastic seismic behavior of the frames have yet to be devised. In the past, we investigated the actual seismic behavior of steel frames with composite beams by means of pseudodynamic testing(3), wherein we used one-bay one-story frames, and emphasis was placed on the effect of the presence or absence of a concrete slab on the earthquake frame behavior. Furthermore, we aimed to clarify how the frames and the beams behaved seismically when the concrete slabs behaved plastically, but did not fail. Thus, in the previous tests, we could not clarify the influence of the compressive failure of the concrete slabs on the frame behavior within the range of large inelastic deformation.

Therefore, the present pseudodynamic tests were performed in order to grasp the frame and beam behavior from the noncompressive to compressive failure domains of the concrete slabs. Furthermore, in the previous study, we analyzed only one-bay one-story frames; however, in this study, two-bay one-story frames were tested in order to elucidate the difference in behavior between two types of composite beams, one joined to an interior column and the other to an exterior column. We also investigated the effect of the presence or absence of a concrete slab on the frame behavior, as well as the relationship between frame ductility and beam ductility. In the pseudodynamic tests, the El Centro NS earthquake (1940) was adopted and its maximum acceleration was amplified to 1.18 or 2.25 times the yield acceleration $s\alpha y$ (the ratio of a yield shear for the story to the mass of the frame) of the frame with a bare steel beam. In addition, in order to obtain the load deformation characteristics of the frames analyzed by the pseudodynamic testing, monotonic and cyclic loading tests were conducted on frames whose shapes were identical to those of the frames used in the pseudodynamic tests. Hereafter, a frame with a concrete slab and a frame without a concrete slab are called "composite beam frame" and "steel beam frame", respectively.

2 EARTHQUAKE BEHAVIOR ANALYSIS BY PSEUDODYNAMIC TEST

Earthquake response analysis was performed on two-bay one-story steel frames with bare steel beams or composite beams. These frames consist of two steel beam frames, SF-1 and SF-2, and two composite beam frames, CF-1 and CF-2. Figure 1 shows a composite beam frame in detail. The

test frames were about one-third the size of full-scale frames. An H-shaped steel beam of H-150x75 x5x7 (beam depth = 150 mm, flange width = 75 mm, web thickness = 5 mm, flange thickness = 7 mm) and an H-shaped steel column of H-175x175x7.5x11 were used to ensure that composite beams failed prior to the steel columns. The slenderness ratio about the weak axis of a half-span of the steel beam was approximately 60. The concrete slab was 910 mm wide and 55 mm thick, and was made of lightweight concrete. The slab width was selected on the basis of the slab effective width in accordance with the Japanese Building Code, the scale factor of the test frames having been taken into consideration. Steel decks, DP-50x40x25x0.8 in size, were oriented perpendicular to the steel beam. The number and spacing of headed studs on the steel beam flange were determined to become fully composite beams. For slab reinforcement, steel bars, 6 mm in diameter, were latticed at a depth of 10 mm from the slab surface with 100 mm spacing. A full penetration butt weld was used to join the beam flange to the column flange, and a fillet weld was used to join the beam web to the column flange. The shape and size of the steel beam frames were the same as those of the composite beam frames without concrete slabs. The geometric properties of the steel beams are shown in Table 1. B/tf, H/tw and l/sry indicate the flange width-to-thickness ratio, web width-to-thickness ratio, and slenderness ratio about the weak axis, respectively. E and W in Table 1 represent the two beams in a frame. Table 1 also shows the full plastic moments sMp of the steel beams. In addition, test types of each specimen are listed in the same table. Table 2 shows the mechanical properties of the flanges and webs of the steel beams obtained from tensile tests on coupons. The table also shows compressive strength Fc of the concrete on cylinder tests.

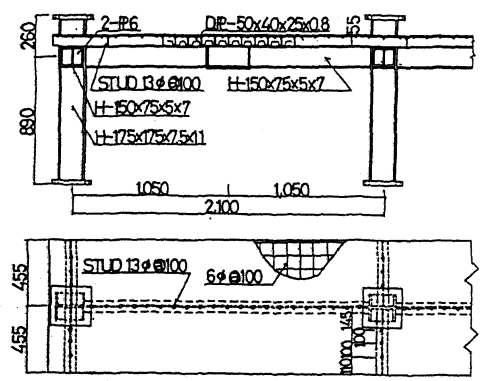

Fig.1 Test specimen of composite beam frame

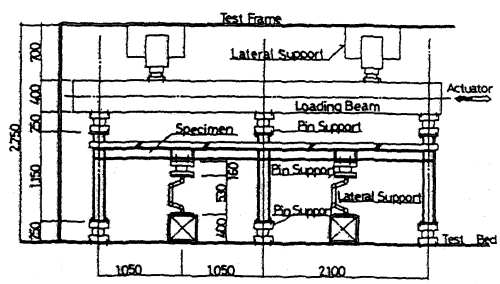

Fig.2 General view of test setup

3 TEST SETUP AND INSTRUMENTATION

Figure 2 illustrates the test setup. The three columns were placed on their pinned supports. The top of each column was prevented from lateral movement, but free rotation about the column axis was allowed. A servo-controlled hydraulic actuator with a dynamic capacity of ±30 ton was installed at the loading beam level. The applied lateral load, which corresponded to the story shear of the frames, was obtained by a load cell attached to the actuator. In order to measure the story displacement of the frames, a displacement meter with maximum stroke of ±100 mm was

Table 1 Geometric property and full plastic moment, and test type

Specimen (Beam)		B/tf	H/tw	l/sry	sMp (kN·m)	Frame	Test Type
SF-1	E	11.5	31.7	58.8	31.5	SBF	Pseudodynamic
SC	W	11.5	31.4	58.8	31.6		Cyclic
SF-2	E	11.5	32.0	58.9	31.0	SBF	Pseudodynamic
	W	11.6	31.8	59.1	30.9		
CF-1	E	11.6	31.9	58.1	31.3	CBF	Pseudodynamic
	W	11.5	32.0	58.0	31.3		
CF-2	E	11.4	32.7	58.2	30.4	CBF	Pseudodynamic
	W	11.5	32.4	58.3	30.4		
SM	E	11.0	30.8	58.7	31.4	SBF	Monotonic
	W	10.9	30.7	58.8	31.5		
CM	E	11.0	30.7	58.7	30.2	CBF	Monotonic
	W	11.1	30.7	58.8	30.0		
CC	E	10.9	30.3	58.7	31.5	CBF	Cyclic
	W	10.9	30.6	58.7	31.3		

Note: SBF=Steel Beam Frame ; CBF=Composite Beam Frame

Table 2 Material property of steel beam and concrete

Specimen (Beam)		σy (N/mm²)	σmax (N/mm²)	εst (x10⁻³)	Est (N/mm²)	εB (%)	Fc (N/mm²)
SF-1	F	307	429	28.6	2226	32.4	–
SC	W	389	472	28.4	2177	21.6	
SF-2	F	301	414	24.4	2403	28.3	–
	W	393	471	28.2	2403	19.5	
CF-1	F	297	428	23.8	2824	30.3	22.6
	W	394	481	27.3	2314	20.6	
CF-2	F	290	404	31.0	2383	31.2	22.4
	W	391	479	27.1	2050	21.5	
SM	F	311	455	23.4	2864	30.0	–
	W	323	466	25.0	2638	33.0	
CM	F	296	434	19.8	2206	29.5	27.1
	W	317	455	25.5	2432	32.9	
CC	F	307	447	23.0	2373	30.7	28.0
	W	322	463	25.7	2873	34.8	

Note: F=Flange; W=Web

set at the surface of the column flange that corresponded to the steel beam axis. In addition, the beam end rotations at the interior and exterior columns were measured. A compact pseudodynamic testing system was constructed using a personal computer. Response analyses, test controlling and data acquisition were carried out integrally through this testing system.

4 NATURAL PERIOD OF FRAME AND GROUND MOTION

The natural period T of steel beam frames SF-1 and SF-2 was set at 0.491 sec. The mass m of the steel beam frames was calculated using the natural period and the measured elastic stiffness K of the frames. The natural period of composite beam frame CF-1 was calculated from its actual lateral stiffness and the mass of frame SF-1. The natural period of frame CF-2 was obtained in the same manner as frame CF-1, using the mass of frame SF-2. The ground motion of the El Centro NS earthquake (1940; duration: 15 sec, including the maximum acceleration 325.72 gal) was used in this test. The maximum acceleration was amplified to 1.18, or 2.25 times the yield acceleration $s\alpha y$ of the steel beam frame. Here, the yield acceleration is defined as the ratio of yield shear for the story to the mass of the frame. Table 3 shows the measured elastic lateral stiffness of each frame, mass, natural period, and maximum acceleration.

5 EQUATION OF MOTION AND DISPLACEMENT CONTROL

The equation of motion was solved by means of the linear acceleration method and then the application of the central difference method in subsequent steps. Since accurate restoring forces cannot be obtained for the beginning of the El Centro NS earthquake due to small response displacements, the linear acceleration method was employed. In the present tests, the linear acceleration method was used from the first step until the step when the response displacement first exceeded approximately 12 % of the yield displacement for the story. The actual elastic lateral stiffness obtained from the static test prior to each pseudodynamic test was used as the required frame stiffness in this method. The integration time interval for both numerical solutions was fixed at 0.01 sec. Viscous damping in proportion to the velocity was considered, and its damping constant was set at 0.2 % of the critical damping.

In this pseudodynamic testing system, the following displacement control method was employed. A small constant displacement was applied to the test frame continually at a specific time interval until the feedback displacement overshot the target displacement. The optimally small constant displacement and the time interval were determined after repeated trial-and-error elastic pseudodynamic tests on frame SF-1. Considering the minimum output of the D/A converter, the optimal displacement and the time interval were 0.0625 mm and 0.3 sec, respectively. The story displacements of steel beam frame SF-1, which were obtained using these control values, are indicated in Fig. 3 by solid lines. Figure 3(a) shows the result at a natural period of 0.491 sec and Fig.3(b), that at 0.296 sec. In the figures, results of the numerical analysis using the measured elastic lateral stiffness are indicated by broken lines. The maximum story displacement by the pseudodynamic test was 1.033 times that of the numerical analysis at a natural period of 0.491 sec, and 1.021 times that at 0.296 sec. There was no phase discrepancy in the response displacement between the pseudodynamic test and the numerical analysis. As stated, when the above control values are used, this testing system is reliable. These values were adopted in the inelastic response analyses.

Table 3 Analyzed frame and ground motion

Frame	K (kN/cm)	m (kN·sec²/cm)	T (sec)	El Centro NS Max. Accel. (gal)
SF-1	93.7	0.572	0.491	1.18sαy(168)
SF-2	95.1	0.581	0.491	2.25sαy(314)
CF-1	147.1	0.572	0.392	1.18sαy(164)
CF-2	139.3	0.581	0.406	2.25sαy(307)

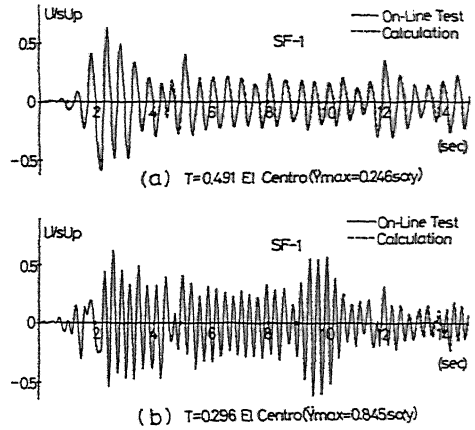

Fig.3 Pseudodynamic test and numerical analysis (elastic response)

6 RESULTS

6.1 Monotonic and cyclic tests on frames

In order to obtain quantitative force deformation characteristics of frames and beams analyzed by the pseudodynamic testing, monotonic and cyclic loading tests were conducted. The shapes of test frames were identical to those of the frames used

in the pseudodynamic test, and the detail of the composite beam frame is shown in Fig.1. The frames were steel beam frame SM and composite beam frame CM for the monotonic test, and steel beam frame SC and composite beam frame CC for the cyclic test. Here, frame SC was the same specimen as frame SF-1 in the pseudodynamic test and was loaded cyclically after the pseudodynamic test. The reason frame SF-1 was used for the cyclic loading test was that the maximum beam ductility of frame SF-1 in the pseudodynamic test was approximately 3.0 and was considered to be within the maximum stable rotation amplitude of the beam.

The relationships between story shear P/sPp and story displacement U/sUp for each frame are shown in Fig.4. The normalization values, sPp and sUp, are obtained by elastic calculation assuming that both beam end moments at exterior columns reach the full plastic moment of the steel beam. The arrows in the figures represent locations of the maximum displacement amplitude of the stable displacement amplitudes. In monotonic tests, frame SM produced the local buckling of flange and lateral buckling of the beam in this order, but the P/sPp-U/sUp relationship was stable at least up to the displacement of 9.6 sUp after bucklings. The story shear of frame CM degraded once because of the compressive failure of the concrete at the maximum story shear. However, the story shear increased once again, and thereafter, the P/sPp-U/sUp relationship was stable at least up to the story displacement of 11.3 sUp. In cyclic tests, the maximum stable displacement amplitude was approximately 3.6 sUp for frame SC and approximately 4.4 sUp for frame CC. The decrease in the story shear was created by a break in the web near the flange for frame SC. With respect to frame CC, the decrease was apparently related to the compressive failure of the concrete and the excessive local buckling of the beam flange. In composite beam frame tests, no lateral buckling deformation of the steel beams was observed.

The relationship between story shear P/sPp and beam end rotation θ/sθp is shown in Fig.5. Here, sθp is defined as sMpl/6EsI (l = beam span between inside surfaces of column flanges; EsI = flexural rigidity of steel beam). The location of the beam end is indicated schematically in each figure. From the results of frame CM in monotonic tests, the beam ductilities at the maximum story shear were found to be 2.52 at the interior column and 2.72 at the exterior column in positive bending regions. These ductilities were 2.45 and 2.92 at the interior and the exterior columns, respectively, in negative bending regions. In cyclic tests, the beam ductilities of frame CC at the maximum stable story displacement amplitude were found to be 5.83 at the interior column and 6.30 at the exterior column in positive bending regions. In negative bending regions, these

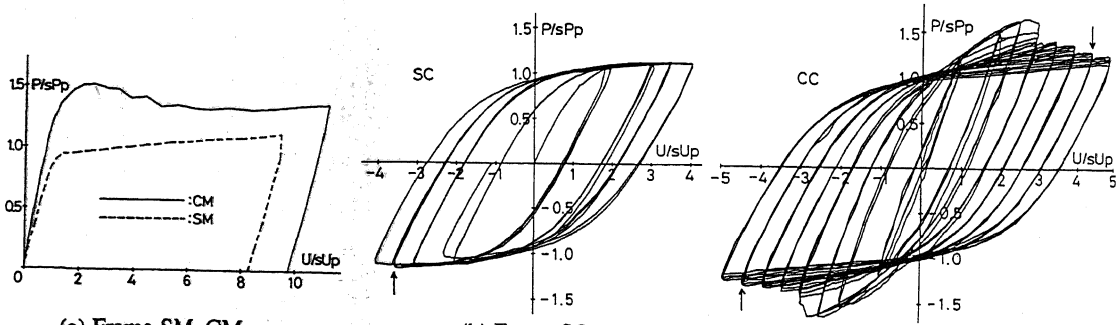

(a) Frame SM, CM (b) Frame SC (c) Frame CC

Fig.4 Story shear vs. story displacement

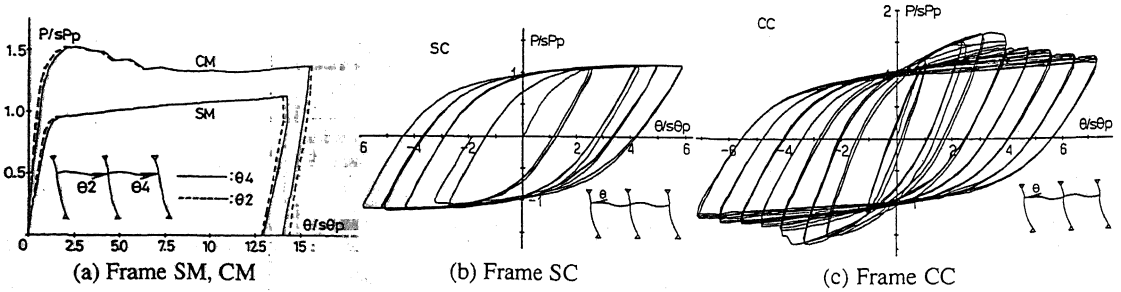

(a) Frame SM, CM (b) Frame SC (c) Frame CC

Fig.5 Story shear vs. beam end rotation

ductilities were 5.72 and 6.64 at the interior and the exterior columns, respectively. With respect to frame SC, these beam ductilities were 4.62 at the interior column and 5.17 at the exterior column.

6.2 Pseudodynamic tests

The responses of story shear P/sPp, story displacement U/sUp and beam end rotation θ/sθp of frames SF-2 and CF-2 are shown in Figs.6 and 7. Here, the beam end rotation represents that at the exterior column. Relationships between the story shear and the story displacement of each frame are presented in Fig.8. Figures 9 and 10 illustrate the maximum response of the story displacement, and the ratio of the maximum beam end rotation at the exterior column to that at the interior column, respectively. At the maximum ground acceleration 1.18 sαy, the concrete slab of frame CF-1 did not fail compressively. The maximum story displacement of frame CF-1 decreased to 1.38 sUp against 2.21 sUp of frame SF-1. The maximum story displacement of frame CF-1 was reduced to

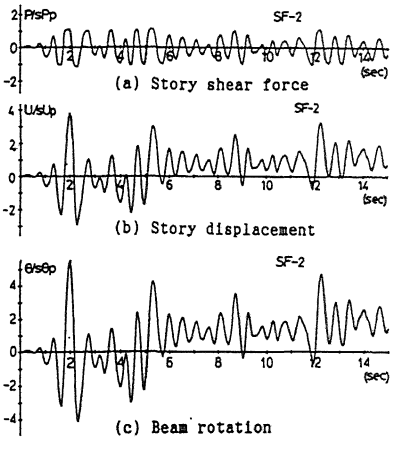

Fig.6 Frame SF-2, T=0.491sec, 2.25sαy

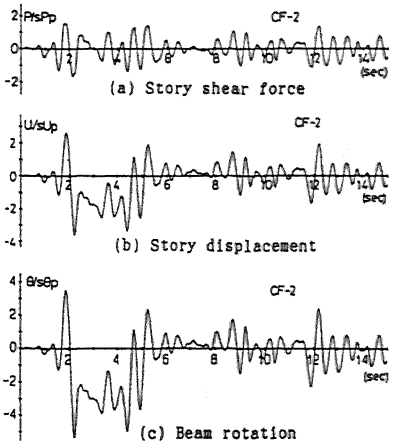

Fig.7 Frame CF-2, T=0.406sec, 2,25sαy

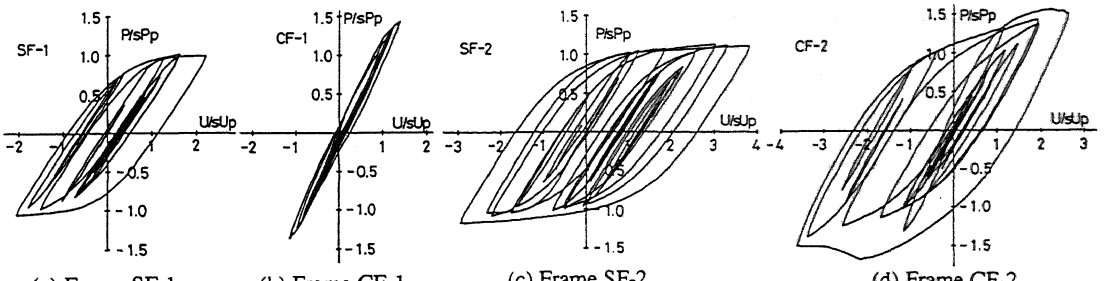

(a) Frame SF-1 (b) Frame CF-1 (c) Frame SF-2 (d) Frame CF-2

Fig.8 Story shear vs. story displacement

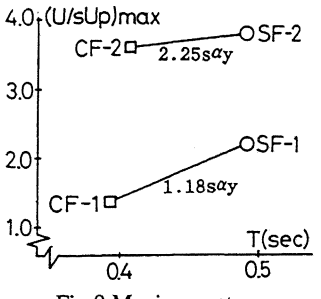

Fig.9 Maximum story displacement

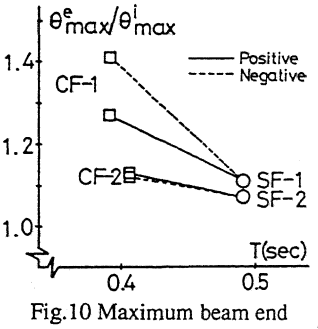

Fig.10 Maximum beam end rotation

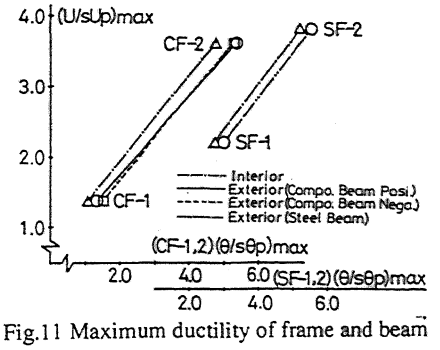

Fig.11 Maximum ductility of frame and beam

approximately 62 % that of frame SF-1, which was identical to a steel beam frame when the concrete slab was removed from frame CF-1. However, when the concrete slab did fail compressively at the maximum ground acceleration 2.25 sαy, the maximum story displacements of frame CF-2 and frame SF-2 were 3.36 sUp and 3.82 sUp, respectively. The ratio of the two maximum story displacements was approximately 0.95 and there was no great difference between the two. When the maximum response story displacement and the maximum stable story displacement amplitude obtained by cyclic tests were compared, both the maximum response story displacements of frames SF-1 and CF-1 at 1.18 sαy ground acceleration were smaller than their maximum stable story displacement amplitudes obtained from the test of frames SC and CC. At 2.25 sαy ground acceleration, the maximum story displacement of frame SF-2 was within the maximum stable story displacement amplitude of frame SC. However, that of frame CF-2 exceeded the maximum stable story displacement amplitude of frame CC.

Regarding beam end rotations, in the case of noncompressive failure of the concrete slab (frame CF-1), the end rotation of the composite beam at the external column increased by approximately 27% that at the interior column in the positive moment region, and approximately 41% in the negative moment region. In the case of compressive failure of the concrete slab (frame CF-2), however, the end rotation of the composite beam at the exterior column increased by approximately 12% over that at the interior column, regardless of the positive or negative moment regions.

Figure 11 shows the relationship between the maximum response ductilities of frames and beams. The upper horizontal axis in the figure represents beam ductilities of frames CF-1 and CF-2, and the lower one the beam ductilities of frames SF-1 and SF-2. At 1.18 sαy ground acceleration, the beam ductilities of frame SF-1 at the exterior and the interior columns were approximately 135 % and 122 % the frame ductility, respectively. However, the beam ductilities at the exterior columns of frame CF-1 were approximately 98 % and 112 % its frame ductility in the positive and negative moment regions, respectively. In particular, beam ductility at the interior column of frame CF-1 was approximately 77 % the frame ductility due to the presence of the concrete slab. In the response at 2.25 sαy ground acceleration, the compressive failure of the concrete slab brought the maximum beam ductilities of frame CF-2 close to those of frame SF-2. Beam ductility of frame CF-2 was approximately 146 % its frame ductility, regardless of positive or negative moment regions.

7 CONCLUSIONS

We clarified seismic behavior of the two-bay one-story composite beam frame and steel beam frame by the pseudodynamic test method. The earthquake acceleration used in the test simulated that of the El Centro NS earthquake (1940). The maximum acceleration was amplified to 1.18 and 2.25 times the yield acceleration of the steel beam frame. The natural period of the steel beam frame was set at 0.491 sec. The natural periods of the composite beam frames were 0.392 sec and 0.406 sec. The following conclusions were reached in the present tests.

1) The presence of the concrete slabs greatly affected the seismic behavior of the frames and the beams.
2) In particular, when the concrete slab did not fail compressively, the difference in response behaviors between the composite beam frame and the steel beam frame was considerable. However, once compressive failure occurred, it produced a maximum response behavior of the composite beam frame which was close to that of the steel beam frame.
3) A relationship between beam ductility and frame ductility was obtained in both the steel beam frame and the compite beam frame. In particular, this relationship was affected by the presence of concrete and the compressive failure of the concrete, which exerted an influence on the restraint of the beam end rotation.
4) In the case of noncompressive failure of the concrete slab, the ratio of increase in beam end rotation at the exterior column to that at the interior column showed a clear difference between the positive and negative moment regions. However, in the case of compressive failure of the concrete slab, the ratio of increase became almost identical in the positive and negative moment regions.

REFERENCES

1. Mukudai, Y., and Matsuo, A. 1983 "A study of the analysis and the behavior of multi-story frames with concrete slab during a severe earthquake." J. Struct. Engrg., Japan, No.29, 211-220(in Japanese)

2. Igarashi, S., Inoue, K., Kim, S.E., and Tada, M. 1984 "A study on elastic-plastic response analysis of framed structures composed of composite beams." Trans., Architectural Institute of Japan, No.337, 39-52(in Japanese)

3. Udagawa, K., and Mimura, H. 1991 "Behavior of composite beam frame by pseudodynamic testing." J. Struct. Engrg., ASCE, Vol.117, No.5, 1317-1335